Biomass Electrocatalysts: Exploiting Haemoglobin-derived Fe Sites Coordinated with S, N-enriched Carbon for Efficient Oxygen Electro-reduction

Nagaraju Shilpa,[§,‡,†] *Jun-Xi Wu,*[§] *Geoffrey I. N. Waterhouse,*[§,‡] *Bicheng Zhu,*[§,‡] *Jadranka Travas-Sejdic,*[§,‡,*] *and David E. Williams*[§,‡,*]

[§]Centre for Innovative Materials and Health, School of Chemical Sciences, The University of Auckland, Private Bag, 92019 Auckland, New Zealand.

[‡]MacDiarmid Institute for Advanced Materials and Nanotechnology, Victoria University of Wellington, PO Box 600, Wellington, New Zealand.

KEYWORDS. Bovine-blood, biomass-derived electrocatalyst, haemoglobin, lignin, tannins, oxygen reduction reaction

ABSTRACT. Biomass resources offer a diverse array of low-cost feedstocks for the manufacture electrocatalysts for the energy sector. In this study, haemoglobin (Hb), lignin, tannic acid and urea were used to develop FeSN/C electrocatalysts comprising iron highly dispersed on S,N-codoped carbon for the oxygen reduction reaction (ORR). By pyrolyzing precursor mixtures containing Hb, lignin, tannic acid and urea in appropriate mass ratios, S,N-codoped carbons with highly dispersed

Fe sites were obtained with ORR performance superior to Pt/C. The developed FeSN/C electrocatalyst exhibited an ORR onset potential of 0.98 V *vs*. RHE in 0.1 M KOH, a half-wave potential ($E_{1/2}$) of 0.87 V and a low Tafel slope of 54 mV/dec. Notably, the electrocatalyst selectively catalysed the 4-electron ORR pathway and exhibited a high methanol tolerance. This work encourages the design of biomass-derived electrocatalysts for oxygen reduction reaction, in particular showing that haemoglobin in bovine blood is a suitable for use an iron source when making Fe-N-C electrocatalysts.

INTRODUCTION

With the continuous advancements in technology, demand for efficient energy conversion and storage technologies, such as fuel cells and rechargeable batteries, is growing rapidly.[1,2] Fuel cells and batteries are critical technologies in the shift away from polluting fossil fuel energy.[3] The oxygen reduction reaction (ORR) is a critical process in the operation of fuel cells and metal-air batteries, with highly active but expensive platinum group metal (PGM) electrocatalysts typically used to drive sluggish 4-electron ORR. The widespread commercialization of fuel cells is intimately linked to production costs, particularly those related to electrode materials.[4,5] Commercialization hinges on the discovery of cost-effective, environmentally friendly, high-performance electrode materials. Consequently, developing electrocatalysts derived from low-cost, green, and renewable feedstocks is garnering increasing importance.[6,7]

Research dedicated to developing electrocatalysts from abundant and readily accessible feedstocks has primarily centred on converting plant-derived biomass into advanced energy materials.[8-12] However, animal processing byproducts also offer useful feedstocks for making catalysts energy conversion systems, though much less work has been done in this area to date.[8] Such approaches have economic benefits, by valorising biomass and minimizing waste. Beyond

its economic and environmental advantages, biomass, with its inherently complex nature, presents diverse molecular structures that can be tailored into functional materials suitable for versatile applications.[13,14] For example, biomass-derived carbon materials exhibit many desirable properties for electrocatalysis, including good wettability, conductivity and chemical stability. Modification of biomass derived carbons with metal active sites enabled electrocatalysts with high catalytic activity, selectivity and durability for many electrochemical processes.[15,16] Recent studies have demonstrated carbon-based ORR electrocatalysts derived from zoomass and phytomass.[17-19] These catalysts typically contain nitrogen (N), sulphur (S), phosphorus (P) heteroatoms, which serve as chelating sites for metals and also boost electrical conductivity.[20-22] Their multifaceted composition gives biomass-derived carbons additional functionality compared to traditional carbon materials used in electrocatalysis (e.g. carbon black or Ketjenblack).

Furthermore, biomass originating from livestock, specifically blood derived from the meat processing industry, is commonly treated as waste and discarded. This blood biomass contains haemoglobin (Hb), comprising four polypeptide chains housing a Fe-porphyrin moiety, rendering it a potential ORR electrocatalyst.[23,24] Consequently, the processing of animal blood biomass holds significant promise for fabricating Fe-based ORR electrocatalysts. Several blood biomass-derived electrocatalysts, prepared using Hb in combination with electrically conductive carbon or carbon nanotubes, have been reported. However, these approaches typically necessitate an additional Fe source and a two-step pyrolysis process to achieve optimal ORR performance.[25-30] The use of an additional Fe source is not desirable, with the development of better electrocatalysts using Hb as the sole Fe source requiring judicious selection of other precursor materials. Lignin, a carbon-rich material, is known to have a favourable interactions with metal ions, making it a suitable material for making catalysts with Hb. Lignin is the most abundant aromatic biopolymer and a renewable

resource produced by the pulping Kraft industry.[31] Its versatility extends to various applications, including serving as a carbon support, catalyst and adsorbent.[32] Recent attention has focused on the π–π stacking interactions and hydrogen bonds between lignin and structurally similar tannins, demonstrating synergistic interactions with metals and underscoring their catalytic potential.[33,34] Notably, tannins (water-soluble polyphenols with a macromolecular structure) have a strong binding affinity to proteins via noncovalent interactions, suggesting they would be useful when making catalysts with proteins like Hb.[35,36]

Herein, we aimed to develop efficient ORR electrocatalysts using haemoglobin, tannic acid and lignin (with urea added as additional N and C source). The precursors were selected due to their low cost and facile processing. We hypothesised that pyrolysis of powder mixtures of Hb, tannic acid, lignin and urea would create S,N-codoped carbons supporting porphyrin-like Fe sites. The S- and N- coordination of Fe on the carbon surface would facilitate electron transfer and boost ORR performance. By benchmarking the performance of the obtained FeSN/C catalysts with a commercial 20 wt.% Pt/C catalyst, we sought to demonstrate the future potential of biomass-derived catalysts in future energy conversion and storage systems.

EXPERIMENTAL SECTION

Materials. Alkali lignin (AL), tannic acid (TA), carbon nanopowder <100 nm particle size (CAS 7440-44-0) and Nafion perfluorinated resin solution (5 wt. % in a mixture of lower aliphatic alcohols and water) were obtained from Sigma-Aldrich. 20 wt.% Pt/C was purchased from the Fuel Cell Store. Urea, NaOH, KOH, ethanol, and isopropyl alcohol (IPA) were obtained from ECP chemicals, New Zealand. All the reagents were of analytical grade and used as received without further purification. Deionised water (Milli-Q, resistivity 18.2 MΩ·cm) was used throughout the

synthesis and experimental processes. Bovine blood was procured from Auckland meat processors to extract haemoglobin (Hb).

Characterisations. Powder X-ray diffraction (XRD) patterns were collected on a PANalytical Empyrean Powder X-ray Diffractometer equipped with a Cu Kα radiation source (λ = 1.5405 Å) and a PIXcel 1D detector. Transmission electron microscopy (TEM) analyses were performed on a FEI Tecnai 12 operating at an acceleration voltage of 120 kV. Atomic force microscopy (AFM) images were collected using a Cypher ES AFM operated in tapping mode. X-ray photoelectron spectroscopy (XPS) data were collected on a Kratos Axis UltraDLD equipped with a hemispherical electron energy analyser. Spectra were excited using monochromatic Al Kα X-rays (1486.69 eV) with the X-ray source operating at 150 W. Scanning electron microscopy (SEM) imaging was performed on a FEI Quanta 200 F with a SiLi (Lithium drifted) EDS detector and a Philips XL30S FEG equipped with a Gattan Alto 2500 cryo unit.

Haemoglobin extraction from bovine blood. The red blood cell (RBC) lysis approach was adopted for Hb extraction.[37] Whole bovine blood from an Auckland meat processor, which contains plasma (55 % of the total blood), white blood cells and platelets (less than 1 % of the total blood) and RBCs (45 % of the total blood), was treated with 10 % sodium citrate and subjected to centrifugation at 3500 rpm for 15 min at 4 °C. The RBC layer was collected and treated with equal volumes of 0.1 % NaCl as a hypotonic solution for 1 h at 4 °C to rupture the RBCs. Next, centrifugation was performed at 3500 rpm for 30 min at 4 °C to remove the RBC membrane debris. Hb located in the supernatant was collected and then freeze-dried to obtain the Hb powder.

Preparation of FeSN/C catalysts. The Fe, S and N-doped carbons (FeSN/C catalysts) were prepared as follows. TA and AL (0.4 g each) were added to 10 mL of water containing 1 mL of 30 wt.% NaOH. The resulting mixture stirred for 30 min at room temperature. Next, 0.8 g of the

freeze-dried Hb powder was added to the tannin and lignin and mixture under constant stirring. 3.2 g of urea was dissolved in 10 mL of water, then slowly added to the Hb dispersion under stirring. The obtained mixture was subjected to ultrasonication for 30 min and then evaporated to dryness on a hot plate at 80 °C for 1 h. The solid residue was then pyrolyzed by heating in air at 250 °C for 2 h (2.5 °C/min) and then 900 °C for 3 h under an argon atmosphere. After cooling to room temperature, the sample was treated with 1 M H_2SO_4 at 80 °C overnight to remove any unstable or loosely bound Fe species from the electrocatalyst's surface. After the acid treatment, the samples were centrifuged, washed thoroughly with water and ethanol, then finally vacuum-dried at 40 °C. The obtained sample, prepared using 16 wt.% Hb powder in the precursor mixture, is denoted herein as FeSN-3/C-3, or simply FeSN/C (Table 1). Further samples were obtained by a similar method with no Hb (SN/C-3) and ca. 9 wt.% Hb (FeSN-2/C-3), respectively. Samples with no urea and only AL were labelled FeS-1/C-3 and FeSN-1/C-2, respectively. A physical mixture of Hb and carbon nanopowder in 1:3 weight ratio was labelled Fe/C-1.

Electrochemical measurements. Electrochemical ORR measurements were conducted in the three-electrode system connected to CH instruments electrochemical workstation. All data were collected in a 0.1 M KOH electrolyte. A Ag/AgCl electrode saturated with KCl and a graphite rod were used as reference and counter electrodes, respectively. Catalyst inks were prepared by adding 5 mg of the catalyst to 1.0 mL of solution containing 576 µL IPA, 384 µL water, and 40 µL of a 5% Nafion solution, followed by ultrasonication for several hours to form a homogeneous ink. The electrocatalysts studied in this work were Fe/C-1, FeSN-1/C-2, FeSN-3/C-3, FeSN-2/C-3, SN/C-3, FeS-1/C-3 and a commercial 20 wt.% Pt/C catalyst. The electrocatalyst ink was dripped onto the surface of a pretreated RDE surface (diameter 0.196 cm^2) and the resulting modified electrodes allowed to dry in air. Catalyst loadings were 0.38 mg/cm^2 for all electrocatalysts.

For the ORR tests, O_2 gas was continuously purged to the 0.1 M KOH electrolyte, and the ORR activities of the electrocatalysts were evaluated in an O_2-saturated electrolyte via cyclic voltammetry (CV) and linear sweep voltammetry (LSV) measurements at scan rate of 50 and 5 mV/s, respectively, using a rotation speed of 1600 rpm.

All potentials in this work were referred to RHE using the Nernst equation:

$$E \text{ (vs. RHE)} = E \text{ (vs. Ag/AgCl)} + 0.1989 + (0.0591 \text{ x pH}) \quad (1)$$

The current density was obtained by normalising the current measured against the geometric area of the electrode, and other ORR activity parameters were obtained from Koutecky-Levich (K-L) plots. In general, the K-L equation is applied to calculate the kinetic current density, number of electrons transferred and Tafel slope of the ORR:[38]

$$\frac{1}{j} = \frac{1}{j_k} + \frac{1}{j_d} \quad (2)$$

$$\frac{1}{j} = \frac{1}{j_k} + \frac{1}{\mathrm{B}\omega^{\frac{1}{2}}} \quad (3)$$

$$\mathrm{B} = 0.2\, n\, F\, D_0^{3/2} C_0\, \nu^{-1/6} \quad (4)$$

where j is the experimentally measured current density, j_d is the diffusion-limiting current density, j_k is the kinetic current density, n is the number of electrons transferred, F is the Faraday constant (96485 C/mol), D_o is the diffusion coefficient of O_2 gas (1.9×10^{-5} cm^2/s), ν is the kinematic viscosity of water (0.01 cm^2/s), C_o is the concentration of O_2 gas in a solution (1.2×10^{-6} mol/cm^3) and ω is the angular rotation of the electrode in rpm.

Tafel slopes were obtained by plotting E *vs.* j_k from the LSV scans at 1600 rpm and 5 mV/s re-arranging the equation (2):

$$j_k = \frac{j * j_d}{j_d - j} \quad (5)$$

From equation (3), a K-L plot of $\frac{1}{j}$ and $\frac{1}{\omega^{\frac{1}{2}}}$ at different potentials gives a linear relation, and the number of electrons transferred can be calculated from the slope using equation (4).

RESULTS AND DISCUSSION

Electrocatalyst characterisation

The fabrication of the FeSN/C electrocatalyst is schematically depicted in Scheme 1. The preparation of FeSN/C involves the utilization of Hb extracted from bovine blood, alkaline lignin (AL), tannic acid (TA) and urea as precursors. We hypothesized that that synergistic interaction between AL and TA with the haem centres in Hb would assist in forming N and S-enriched carbon structures supporting Fe single atom sites. Urea was added as an additional nitrogen source and as a porosity promoter. We varied the amounts of the different biomass components and urea to explore the effect of electrocatalyst composition and structure on ORR performance. Table 1 lists the amount of each precursor used for synthesis of each catalyst.

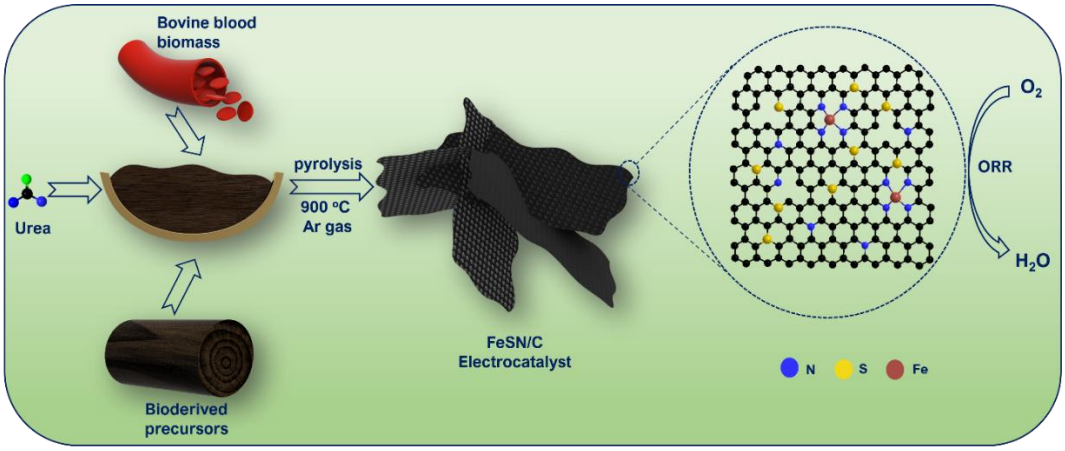

Scheme 1. Schematic illustration of FeSN/C electrocatalyst preparation from various biomass feedstocks.

Figure 1a-c shows transmission electron microscopy (TEM) images for the FeSN/C (i.e. FeSN-3/C-3 catalyst). The images show the sample consisted to nanostructured carbon sheets, with no obvious metallic Fe nanoparticles present on the carbon sheets. Field-emission scanning electron microscopy (FESEM) images in Figure S1 verified the rough and non-uniform morphology of the carbon sheets. The corresponding energy-dispersive X-ray spectroscopy (EDS) spectrum (Figure S2) confirmed the presence of C, N, O, S and Fe in the FeSN/C electrocatalyst.

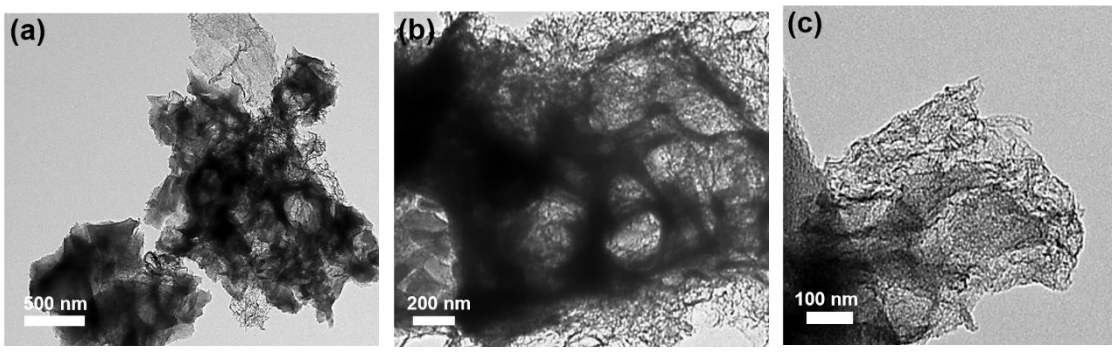

Figure 1. (a, b, c) TEM images of FeSN/C electrocatalyst (specifically FeSN-3/C-3) at different magnifications.

X-ray diffraction (XRD) patterns for the FeSN/C and SN/C catalysts (Figure S3) showed broad diffraction peaks corresponding to the (002) and (100) planes of carbon, indicative the heteroatom-doped carbon support possessed a defective or amorphous nature.[39,40] Data for the FeSN/C and SN/C catalysts were near identical. No peaks due to Fe^0 or FeO_x phases were seen by XRD for the FeSN/C catalysts, suggesting that any Fe in the sample was likely atomically-dispersed in porphyrin-like sites. Additional surface morphological analysis using AFM was conducted to examine surface roughness, as depicted in Figures 2a,b and Figure S4. Visual inspection of material 2D and 3D AFM images reveals finer-grained features of FeSN/C (Figures 2a,b) compared to SN/C (Figures S4c,d). The root mean square (RMS) roughness values of SN/C and FeSN/C were ca. 9 and ca. 12 nm, respectively. These values suggest that FeSN/C has rougher

surface features than SN/C. Such structural differences were expected to play a role in the electrocatalysis, with a rough surface enhancing the ORR performance.[41]

Table 1. Approximate composition of precursors mixtures used to prepare the different electrocatalysts.

Electrocatalyst	Haemoglobin (Hb), wt.%	Tannic acid (TA), wt.%	Alkaline lignin (AL), wt.%	Urea, wt.%
Fe/C-1	16	physical mixture of Hb and carbon nanopowder (84)		
FeSN-1/C-2	4	0	19	76
SN/C-3	0	10	10	80
FeS-1/C-3	2	49	49	0
FeSN-2/C-3	9	9	9	72
FeSN-3/C-3	16	8	8	66

C-1: commercial carbon nanopowder, C-2: only lignin, C-3: lignin and tannin

X-ray photoelectron spectroscopy (XPS) was employed to analyse the near-surface region chemical composition of the FeSN/C electrocatalyst. The XPS survey spectrum revealed that the presence of C, N, O, S and Fe in the FeSN/C electrocatalyst (Figure S5). The C 1*s* spectrum for FeSN/C (Figure 2c) showed peaks at 284.4, 285.5, 287.8 and 290.6 eV which could readily be assigned to C-C/C=C, C-N/C-S, -CO_2H and π-π* shake-up satellites, respectively. The N 1*s* spectrum of FeSN/C (Figure 2d) was deconvoluted into six peaks at 397.9, 398.9, 399.8, 400.9, 402.3 and 403.8 eV, which could readily be assigned to pyridinic N, Fe-N_x, pyrrolic N, graphitic N and two distinct N-oxide species, respectively.[42] Pyridinic N and graphitic N were dominant N species in the sample, both of which are known to be beneficial for boosting ORR activity. The S 2*p* spectrum for FeSN/C (Figure 2e) showed peaks at 163.6, 164.8, 167.4, and 168.5 eV. The set of peaks at 163.6 and 164.8 eV (2:1 area ratio) were assigned to the S $2p_{3/2}$ and S $2p_{1/2}$ signals, respectively, of a sulfide species (S^{2-}) codoped with nitrogen in the carbon support.[43]

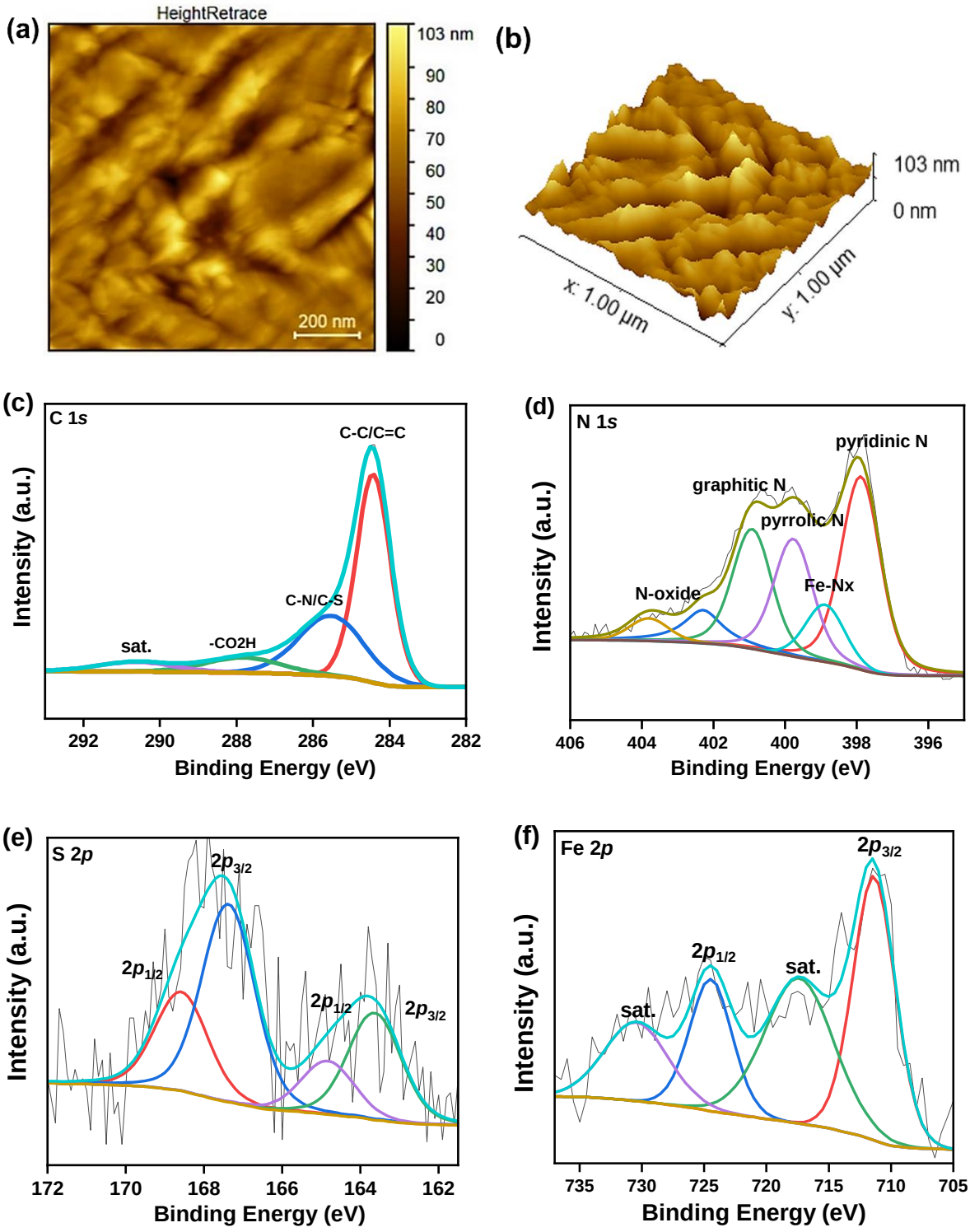

Figure 2. AFM images of FeSN-3/C-3 in 2D (a) and 3D view (b). XPS core-level spectra of FeSN-3/C-3: (c) C 1*s* spectrum, (d) N 1*s* spectrum, (e) S 2*p* spectrum, and (f) Fe 2*p* region.

The 167.4 and 168.5 eV peaks (2:1 area ratio) were assigned to the S $2p_{3/2}$ and S $2p_{1/2}$ signals, respectively, of a more oxidized sulfur species, likely sulfite, formed through air oxidation of sulfide. The high-resolution Fe 2*p* XPS spectrum (Figure 2f) contained two sets of peaks. Peaks at 711.4 and 724.5 eV (2:1 area ratio) were assigned to the Fe $2p_{3/2}$ and Fe $2p_{1/2}$ signals, respectively, of a Fe^{2+} or Fe^{3+} species. A further set of peaks at higher binding energy, 717.4 eV (Fe $2p_{1/2}$) and 730.5 eV (Fe $2p_{1/2}$), are iron shake-up satellites.[44] The XPS data thus shows that the FeSN/C catalyst contained a N,S-codoped carbon support rich in Heme-like (Fe-N_x) sites. Accordingly, the catalyst was expected to offer excellent performance for the ORR in alkaline media.

Electrochemical performance

The electrocatalytic ORR performance of the different electrocatalysts were assessed using a rotating disc electrode (RDE) in a 0.1 M KOH electrolyte. Cyclic voltammetry (CV) and linear scan voltammetry (LSV) measurements were conducted, employing the coated glassy carbon electrode, graphite rod and Ag/AgCl as the working, counter, and reference electrodes, respectively. The CV curves comparing O_2-saturated and N_2-saturated electrolytes clearly show significant ORR electrocatalytic activity on a high surface area electrode (Figure S6). Figure 3a shows the LSV profiles of the Fe/C-1, FeSN-1/C-2, FeS/C-3, SN/C-3, FeSN-2/C-3, FeSN-3/C-3 and 20% Pt/C electrocatalysts, recorded at an electrode rotation speed of 1600 rpm and a scan rate of 5 mV/s. The FeSN-3/C-3electrocatalyst exhibited an onset potential of 0.98 V, comparable to Pt/C. In contrast, the onset of oxygen reduction on Fe/C-1, FeSN-1/C-2, FeS/C-3, SN/C-3, and FeSN-2/C-3 were observed at lower potentials of 0.70 V, 0.84 V, 0.77 V, 0.86 V and 0.90 V, respectively. These values are higher by 280 mV, 140 mV, 210 mV, 120 mV and 80 mV, respectively, compared to FeSN-3/C-3. The half-wave potential ($E_{1/2}$) of FeSN-3/C-3 was 0.87 V

(Figure 3b), outperforming Pt/C ($E_{1/2}$ = 0.83 V) and the other catalysts: FeSN-2/C-3 (0.78 V), SN/C-3 (0.74 V), FeSN-1/C-2 (0.64 V), FeS/C-3 (0.63 V) and Fe/C-1 (0.49 V).

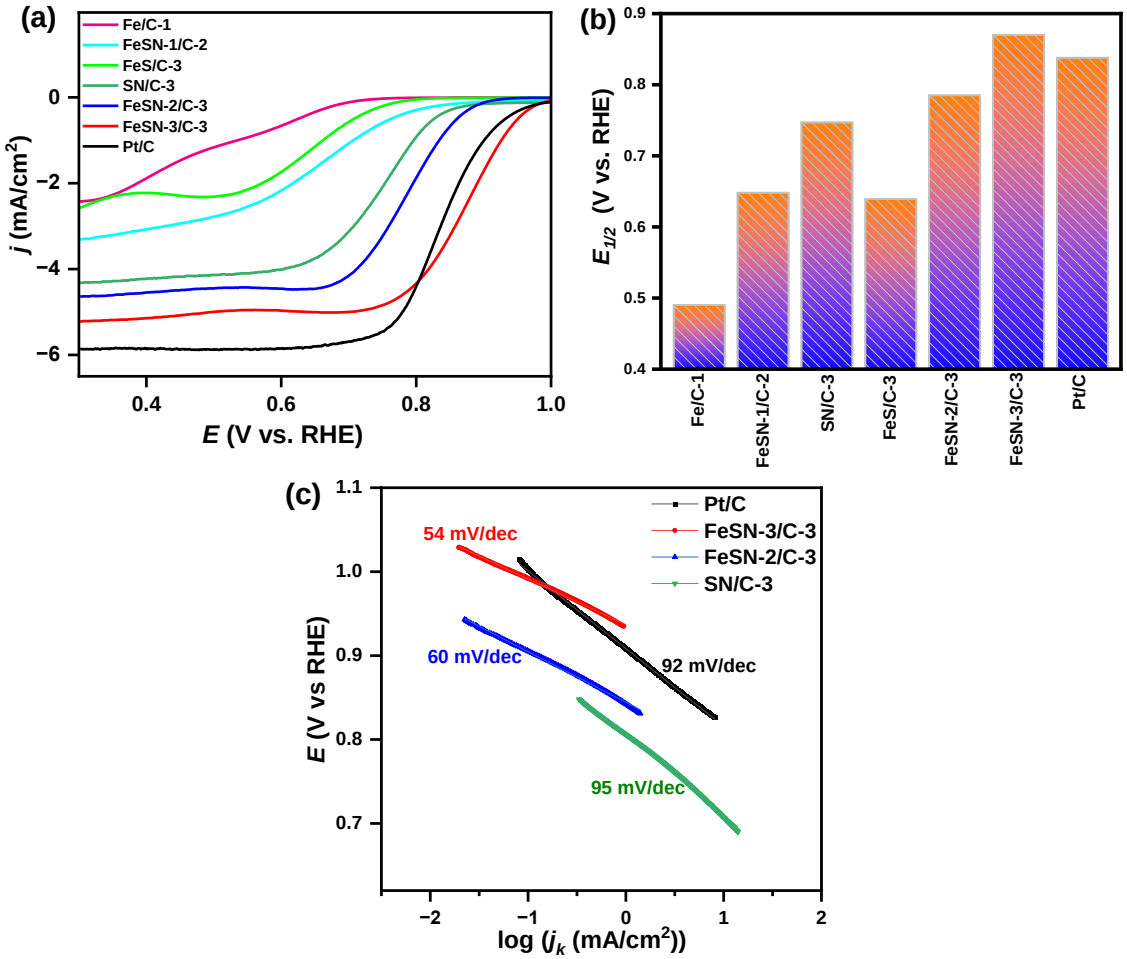

Figure 3. (a) ORR catalytic performance of Fe/C-1, FeSN-1/C-2, FeS/C-3, SN/C-3, FeSN-2/C-3, FeSN-3/C-3, and Pt/C in an O_2-saturated 0.1 M KOH solution with a rotation rate of 1600 rpm. (b) Comparison of the half-wave potential of the various electrocatalysts. (c) Tafel slopes of SN/C-3, FeSN-2/C-3, FeSN-3/C-3, and Pt/C.

During the electrocatalytic testing, we noticed that the Fe/C-1 catalyst was very susceptible to catalyst detachment from the electrode surface during ORR measurements. Similarly, the samples lacking the stabilizing effect of carbon, pore generator (urea) and good interactions between haem with carbon, namely FeSN-1/C-2, FeS/C-3, and Fe/C-1, also delivered poor ORR performance

compared to FeSN-3/C-3. This outstanding ORR performance of the FeSN-3/C-3 electrocatalyst compared to the other reference electrocatalysts investigated in this work highlights the importance of the correct proportions of biomass feedstocks and urea in the pyrolysis precursor mixture, which ultimately allows the fabrication of heteroatom-enriched carbons rich in exposed Fe active sites. The ORR kinetics were further investigated through Tafel plots, as shown in Figure 3c. The low Tafel slopes measured for FeSN-3/C-3 (60 mV/dec) and FeSN-2/C-3 (54 mV/dec) indicate a more facile ORR mechanism compared to Pt/C (92 mV/dec) and SN/C-3 (95 mV/dec).

Polarization curves of FeSN-3/C-3 at various electrode rotation speeds are illustrated in Figure S7, revealing an increase in current density with the increase in electrode rotation speed. The K-L plots obtained by plotting the current density inversion ($1/j$) against the inversion square root of the angular velocity inversion ($1/\omega^{1/2}$) at different potentials (Figure 4a) demonstrate linear behaviour. The slope (1/B) of these lines indicates first-order kinetics on FeSN-3/C-3 with respect to the dissolved O_2 concentration. The K-L equation and its kinetic parameters are detailed in the electrochemical measurement section. The electron transfer number ("n") during the ORR for FeSN-3/C-3 was approximately 4 at potentials ranging from 0.3 V to 0.7 V potentials (Figure 4b). This suggests that FeSN-3/C-3 possessed good selectivity for O_2 reduction to water *via* 4-electron pathways, indicating negligible H_2O_2 formation. Thus, FeSN-3/C-3 offers a surface with a judicious combination of active sites that are capable of driving dioxygen reduction efficiently through the favoured four-electron pathway. Notably, the significant differences were observed between the control samples and FeSN-3/C-3 regarding ORR activity and kinetic pathways, suggesting efficient electron transfer between the Fe sites and N, S enriched carbon support in FeSN-3/C-3.

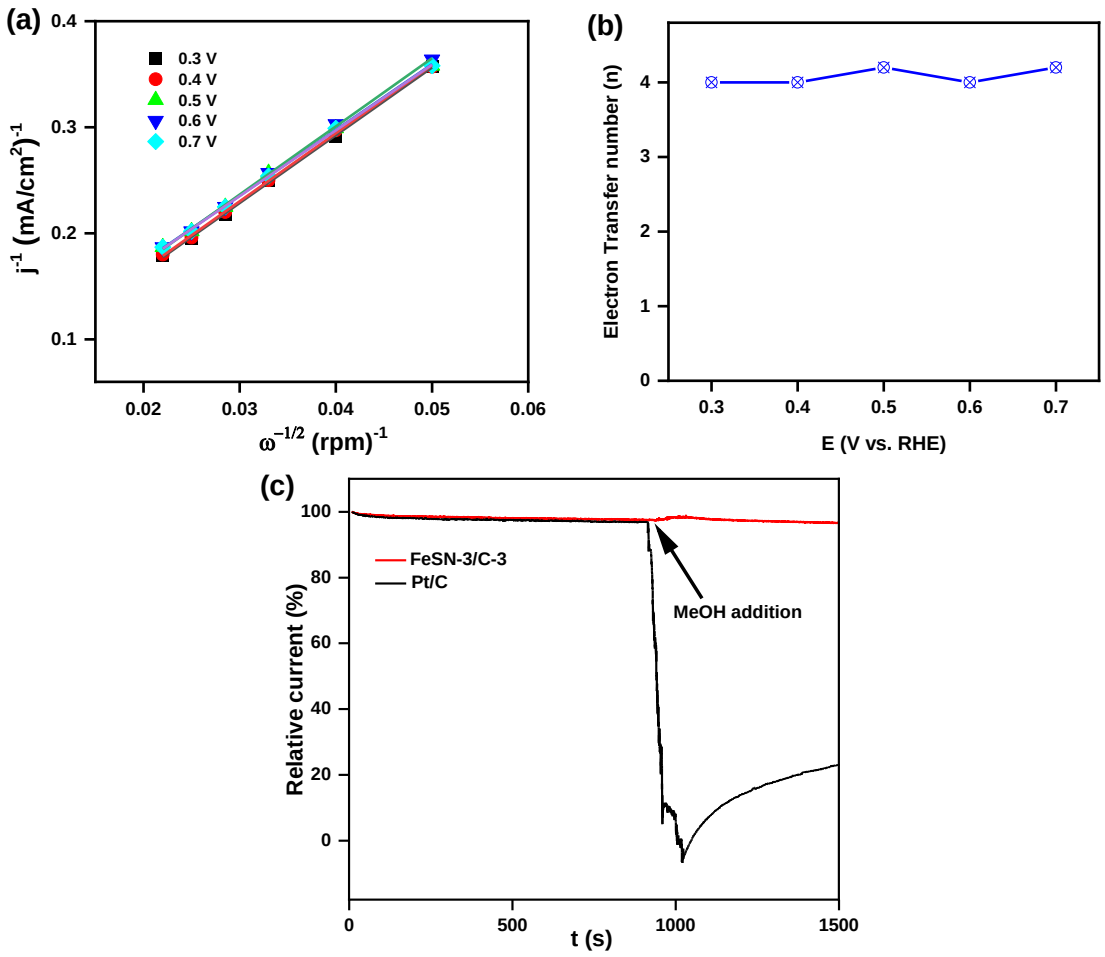

Figure 4. (a) K-L plots and (b) number of electrons of FeSN-3/C-3 during ORR respectively. (c) Chronoamperometric curves showing methanol tolerance of FeSN-3/C-3 and Pt/C at 0.7 V.

The kinetic current density (j_k) value at 0.80 V, calculated using the K-L equation for FeSN-3/C-3 (27 mA cm^{-2}), surpassed that of 20% Pt/C (17 mA cm^{-2}). The j_k values for FeSN-2/C-3 and SN/C-3 were 3.0 mA cm^{-2} and 1.1 mA cm^{-2}, respectively. The mass activity of the electrocatalysts at 0.80 V followed the order FeSN-3/C-3 (70 A/g) > FeSN-2/C-3 (8.6 A/g) > SN/C-3 (2.8 A/g), with the mass activity of the Pt/C catalyst estimated to be 68 A/g. The data further confirmed that FeSN-3/C-3 was comparable, even surpassing, Pt/C in terms of ORR performance.

An accelerated durability test (ADT) was conducted on FeSN-3/C-3 by subjecting the material to 1600 cycles between 0.6 to 1.0 V *vs*. RHE. Figure S8 displays the polarisation curve of FeSN-

3/C-3 after the ADT, revealing a very slight shift in the onset and half-wave potentials of only 20 mV, suggesting good operational stability. When utilizing methanol as a fuel source in direct methanol fuel cells (DMFCs), an ORR electrocatalysts tolerance to methanol is an important consideration. Methanol crossover from the anode to the cathode can compromise the electrocatalyst's activity, reducing the cell voltage.[45] Consequently, the methanol tolerance of FeSN-3/C-3 and the commercial Pt/C catalyst during ORR were evaluated by introducing 5% methanol into the 0.1 M KOH electrolyte and monitoring the corresponding changes in current over time. Figure 4c shows that the steady current response of FeSN-3/C-3 was not affected by adding methanol, whereas the current response of Pt/C decreased dramatically in the presence of methanol. The suggests that ORR on FeSN-3/C-3 was not affected by reaction intermediates of the methanol oxidation reaction, whereas the Pt/C electrocatalyst was poisoned under the same conditions.

CONCLUSIONS

Our study demonstrates the successful use of bovine blood haemoglobin as a source of iron porphyrin for preparing FeSN/C electrocatalysts. By utilizing haemoglobin, tannic acid, lignin and urea as precursors, a FeSN/C catalyst with superior ORR onset and superior half-wave potentials compared to a commercial Pt/C catalyst was obtained. The sulphur and nitrogen co-doping of the carbon support markedly enhanced the ORR electrocatalytic activity. Electrochemical investigations further revealed that FeSN/C promoted the desired 4-electron pathway with minimal H_2O_2 formation, whilst also offering a high methanol tolerance suggesting a possible end-use in DMFCs. This work provides a rational approach for designing ORR electrocatalysts from biomass feedstocks. In most parts of the world, bovine blood is a waste product of meat processing. Here

we showed it offers a valuable building block in the design of non-precious metal electrocatalysts for energy conversion and storage.

ASSOCIATED CONTENT

Supporting Information. SEM images, EDS spectrum, XRD patterns, AFM images, XPS survey graph, electrochemical measurements and electrocatalyst activity comparison table. (PDF) The supporting information file is available free of charge.

AUTHOR INFORMATION

Corresponding Author

*Email for David Williams: david.williams@auckland.ac.nz

*Email for Jadranka Travas-Sejdic: j.travas-sejdic@auckland.ac.nz

Present Addresses

[†]DTU Energy, Technical University of Denmark, Fysikvej, DK-2800 Kgs. Lyngby, Denmark

Notes

The authors declare no competing financial interest.

ACKNOWLEDGMENT

We acknowledge the support from The University of Auckland (Faculty of Science and Faculty of Engineering) and the MacDiarmid Institute for Advanced Materials and Nanotechnology.

REFERENCES

1. Lund, H. Renewable energy strategies for sustainable development. *Energy* **2007**, *32*, 912-919.

2. Shao, C.; Zhao, Y.; Qu, L. Recent advances in highly integrated energy conversion and storage system. *SusMat.* **2022**, *2*, 142-160.

3. Dresselhaus, M. S.; Thomas, I. L. Alternative energy technologies. *Nature* **2001**, *414*, 332-337.

4. Zaman, S.; Huang, L.; Douka, A. I.; Yang, H.; You, B.; Xia, B. Y. Oxygen Reduction Electrocatalysts toward Practical Fuel Cells: Progress and Perspectives. *Angew. Chem. Int. Ed.* **2021**, *60*, 17832-17852.

5. Wang, X. X.; Swihart, M. T.; Wu, G. Achievements, challenges and perspectives on cathode catalysts in proton exchange membrane fuel cells for transportation. *Nat. Catal.* **2019**, *2*, 578-589.

6. Zhu, C.; Li, H.; Fu, S.; Du, D.; Lin, Y. Highly efficient nonprecious metal catalysts towards oxygen reduction reaction based on three-dimensional porous carbon nanostructures. *Chem. Soc. Rev.* **2016**, *45*, 517-531.

7. Xia, W.; Mahmood, A.; Liang, Z.; Zou, R.; Guo, S. Earth-Abundant Nanomaterials for Oxygen Reduction. *Angew. Chem. Int. Ed.* **2016**, *55*, 2650-2676.

8. Borghei, M.; Lehtonen, J.; Liu, L.; Rojas, O. J. Advanced Biomass-Derived Electrocatalysts for the Oxygen Reduction Reaction. *Adv. Mater.* **2018**, *30*, 1703691.

9. Liu, T.; Yabu, H. Biomass-Derived Electrocatalysts: Low-Cost, RobustMaterials for Sustainable Electrochemical Energy Conversion. *Adv. Energy Sustainability Res.* **2024**, *5,* 2300168.

10. Sekhon, S. S.; Lee, J.; Park, J.-S. Biomass-derived bifunctional electrocatalysts for oxygen reduction and evolution reaction: A review. *J. Energy Chem.* **2022**, *65*, 149-172.

11. Dessalle, A.; Quílez-Bermejo, J.; Fierro, V.; Xu, F.; Celzard, A. Recent progress in the development of efficient biomass-based ORR electrocatalysts. *Carbon* **2023**, *203*, 237-260.

12. Park, S.; Kim, J.; Kwon, K. A review on biomass-derived N-doped carbons as electrocatalysts in electrochemical energy applications. *Chem. Eng. J.* **2022**, *446*, 137116.

13. Zhang, G.; Liu, X.; Wang, L.; Fu, H. Recent advances of biomass derived carbon-based materials for efficient electrochemical energy devices. *J. Mater. Chem. A* **2022**, *10*, 9277-9307.

14. Feng, Y.; Jiang, J.; Xu, Y.; Wang, S.; An, W.; Chai, Q.; Prova, U. H.; Wang, C.; Huang, G. Biomass derived diverse carbon nanostructure for electrocatalysis, energy conversion and storage. *Carbon* **2023**, *211*, 118105.

15. Shetty, A.; Molahalli, V.; Sharma, A.; Hegde, G. Biomass-Derived Carbon Materials in Heterogeneous Catalysis: A Step towards Sustainable Future. *Catalysts* **2023**, *13*, 20.

16. He, H.; Zhang, R.; Zhang, P.; Wang, P.; Chen, N.; Qian, B.; Zhang, L.; Yu, J.; Dai, B. Functional Carbon from Nature: Biomass-Derived Carbon Materials and the Recent Progress of Their Applications. *Adv. Sci.* **2023**, 2205557.

17. Das, S.; Ghosh, S.; Kuila, T.; Murmu, N. C.; Kundu, A. Biomass-Derived Advanced Carbon-Based Electrocatalysts for Oxygen Reduction Reaction. *Biomass* **2022**, *2*, 155-177.

18. Jiang, M.; Yu, X.; Yang, H.; Chen, S. Optimization Strategies of Preparation of Biomass-Derived Carbon Electrocatalyst for Boosting Oxygen Reduction Reaction: A Minireview. *Catalysts* **2020**, *10*, 1472.

19. Cao, Y.; Sun, Y.; Zheng, R.; Wang, Q.; Li, X.; Wei, H.; Wang, L.; Li, Z.; Wang, F.; Han, N. Biomass-derived carbon material as efficient electrocatalysts for the oxygen reduction reaction. *Biomass and Bioenergy* **2023**, *168*, 106676.

20. Gao, S.; Fan, H.; Zhang, S. Nitrogen-enriched carbon from bamboo fungus with superior oxygen reduction reaction activity. *J. Mater. Chem. A* **2014**, *2*, 18263-18270.

21. Song, M. Y.; Park, H. Y.; Yang, D.-S.; Bhattacharjya, D.; Yu, J.-S. Seaweed-Derived Heteroatom-Doped Highly Porous Carbon as an Electrocatalyst for the Oxygen Reduction Reaction. *ChemSusChem* **2014**, *7*, 1755-1763.

22. Guo, C.-Z.; Liao, W.-L.; Chen, C.-G. Design of a non-precious metal electrocatalyst for alkaline electrolyte oxygen reduction by using soybean biomass as the nitrogen source of electrocatalytically active center structures. *J. Power Sources* **2014**, *269*, 841-847.

23. Jiang, W.-J.; Hu, W.-L.; Zhang, Q.-H.; Zhao, T.-T.; Luo, H.; Zhang, X.; Gu, L.; Hu, J.-S.; Wan, L.-J. From biological enzyme to single atomic Fe-N-C electrocatalyst for efficient oxygen reduction. *Chem. Commun.* **2018**, *54*, 1307-1310.

24. Maruyama, J.; Abe, I. Carbonized Hemoglobin Functioning as a Cathode Catalyst for Polymer Electrolyte Fuel Cells. *Chem. Mater.* **2006**, *18*, 1303-1311.

25. Guo, C.; Liao, W.; Li, Z.; Chen, C. Exploration of the catalytically active site structures of animal biomass-modified on cheap carbon nanospheres for oxygen reduction reaction with high activity, stability and methanol-tolerant performance in alkaline medium. *Carbon* **2015**, *85*, 279-288.

26. Zheng, J.; Guo, C.; Chen, C.; Fan, M.; Gong, J.; Zhang, Y.; Zhao, T.; Sun, Y.; Xu, X.; Li, M.; Wang, R.; Luo, Z.; Chen, C. High content of pyridinic- and pyrrolic-nitrogen-modified carbon nanotubes derived from blood biomass for the electrocatalysis of oxygen reduction reaction in alkaline medium. *Electrochim. Acta* **2015**, *168*, 386-393.

27. Zhang, J.; Li, Q.; Zhang, C.; Mai, L.; Pan, M.; Mu, S. A N-self-doped carbon catalyst derived from pig blood for oxygen reduction with high activity and stability. *Electrochim. Acta* **2015**, *160*, 139-144.

28. Guo, C.-Z.; Chen, C.-G.; Luo, Z.-L. A novel nitrogen-containing electrocatalyst for oxygen reduction reaction from blood protein pyrolysis. *J. Power Sources* **2014**, *245*, 841-845.

29. Lee, J.; Kim, H. S.; Jang, J.-H.; Lee, E.-H.; Jeong, H.-W.; Lee, K.-S.; Kim, P.; Yoo, S. J. Atomic-Scale Engineered Fe Single-Atom Electrocatalyst Based on Waste Pig Blood for High-Performance AEMFCs. *ACS Sustainable Chem. Eng.* **2021**, *9*, 7863-7872.

30. Maruyama, J.; Hasegawa, T.; Iwasaki, S.; Kanda, H.; Kishimoto, H. Heat Treatment of Carbonized Hemoglobin with Ammonia for Enhancement of Pore Development and Oxygen Reduction Activity. *ACS Sustainable Chem. Eng.* **2014**, *2*, 493-499.

31. Duval, A.; Lawoko, M. A review on lignin-based polymeric, micro- and nano-structured materials. *React. Funct. Polym.* **2014**, *85*, 78-96.

32. Upton, B. M.; Kasko, A. M. Strategies for the Conversion of Lignin to High-Value Polymeric Materials: Review and Perspective. *Chem. Rev.* **2016**, *116*, 2275-2306.

33. Afewerki, S.; Edlund, U. Combined Catalysis: A Powerful Strategy for Engineering Multifunctional Sustainable Lignin-Based Materials. *ACS Nano* **2023**, *17*, 7093-7108.

34. Guo, X.; Jiang, Z.; Ma, Y.; Fan, J.; Clark, J. H.; Zhang, W.; Shi, B. Co-self-assembly of lignin and tannin: A novel catalyst support for hydrogenation of lignin-derived aldehydes. *Appl. Catal. B* **2023**, *339*, 123175.

35. Lei, Y.; Tang, Z.; Liao, R.; Guo, B. Hydrolysable tannin as environmentally friendly reducer and stabilizer for graphene oxide. *Green Chem*. **2011**, *13*, 1655-1658.

36. Lin, D.; Xing, B. Tannic Acid Adsorption and Its Role for Stabilizing Carbon Nanotube Suspensions. *Environ. Sci. Technol.* **2008**, *42*, 5917-5923.

37. Jayawardena, N.; Kaur, M.; Nair, S.; Malmstrom, J.; Goldstone, D.; Negron, L.; Gerrard, J. A.; Domigan, L. J. Amyloid Fibrils from Hemoglobin. *Biomolecules* **2017**, *7*, 37.

38. Bhuvanendran, N.; Ravichandran, S.; Xu, Q.; Maiyalagan, T.; Su, H. A quick guide to the assessment of key electrochemical performance indicators for the oxygen reduction reaction: A comprehensive review. *Int. J. Hydrog. Energy* **2022**, *47*, 7113-7138.

39. Wang, J.; Zhang, Q.; Deng, M. Eco-Friendly Preparation of Biomass-Derived Porous Carbon and Its Electrochemical Properties. *ACS Omega* **2022**, *7*, 22689-22697.

40. Ramesh, T.; Rajalakshmi, N.; Dhathathreyan, K. S.; Reddy, L. R. G. Hierarchical Porous Carbon Microfibers Derived from Tamarind Seed Coat for High-Energy Supercapacitor Application. *ACS Omega* **2018**, *3*, 12832-12840.

41. Sharma, R.; Kar, K. K. Effects of Surface Roughness and N-content on Oxygen Reduction Reaction Activity for the Carbon-based Catalyst Derived from Poultry Featherfiber. *Electrochim. Acta* **2016**, *191*, 876-886.

42. Fu, X.; Li, N.; Ren, B.; Jiang, G.; Liu, Y.; Hassan, F. M.; Su, D.; Zhu, J.; Yang, L.; Bai, Z.; Cano, Z. P.; Yu, A.; Chen, Z. Tailoring FeN4 Sites with Edge Enrichment for Boosted Oxygen Reduction Performance in Proton Exchange Membrane Fuel Cell. *Adv. Energy Mater.* **2019**, *9*, 1803737.

43. Hu, K.; Tao, L.; Liu, D.; Huo, J.; Wang, S. Sulfur-Doped Fe/N/C Nanosheets as Highly Efficient Electrocatalysts for Oxygen Reduction Reaction. *ACS Appl. Mater. Interfaces* **2016**, *8*, 19379-19385.

44. Velázquez-Palenzuela, A.; Zhang, L.; Wang, L.; Cabot, P. L.; Brillas, E.; Tsay, K.; Zhang, J. Carbon-Supported Fe-Nx Catalysts Synthesized by Pyrolysis of the Fe(II)-2,3,5,6-Tetra(2-pyridyl)pyrazine Complex: Structure, Electrochemical Properties, and Oxygen Reduction Reaction Activity. *J. Phys. Chem. C* **2011**, *115*, 12929-12940.

45. Martinaiou, I.; Videla, A. H. A. M.; Weidler, N.; Kubler, M.; Wallace, W. D. Z.; Paul, S.; Wagner, S.; Shahraei, A.; Stark, R. W.; Specchia, S.; Kramm, U. I. Activity and degradation study of an Fe-N-C catalyst for ORR in Direct Methanol Fuel Cell (DMFC). *Appl. Catal. B*: *Environmental* **2020**, *262*, 118217.

SYNOPSIS (Word Style “SN_Synopsis_TOC”).